Acta metall. mater. Vol. 39, No. 8, pp. 1883–1890, 1991
Printed in Great Britain.

0956-7151/91 $3.00 + 0.00

MATRIX CRACKING IN INTERMETALLIC COMPOSITES CAUSED BY THERMAL EXPANSION MISMATCH

T. C. LU[1], J. YANG[1], Z. SUO[1], A. G. EVANS[1], R. HECHT[3] and R. MEHRABIAN[1,2]

[1]Materials Department and Mechanical Engineering Department, University of California, Santa Barbara, CA 93106, [2]Carnegie Mellon University, Pittsburgh, PA 15213 and [3]Pratt and Whitney Aircraft, West Palm Beach, FL 33410, U.S.A.

(Received 24 July 1990; in revised form 24 January 1991)

Abstract—Matrix cracking in brittle matrix composites caused by thermal expansion misfit has been addressed by a combination of experiment with calculations. It has been established that a critical reinforcement size exists below which matrix cracking is suppressed. This concept is summarized in terms of a non-dimensional group $\mathscr{R}$, of the reinforcement size, misfit strain, elastic modulus and matrix toughness. It has also been demonstrated that the interface exerts a major influence on matrix cracking, through relaxation of constraint by debonding. Furthermore, the results imply that a failsafe value of $\mathscr{R}$ exists, of order unity, that can be used to select material combinations that suppress matrix cracking.

Résumé—En combinant l'expérience aux calculs, on s'est attaqué à la fissuration de la matrice—dans les composites à matrice fragile—due à un désaccord de dilatation thermique. Il existe une taille critique des renforts au-dessous de laquelle il n'y a plus de fissuration de la matrice. Ce concept est résumé sous forme d'un groupe sans dimension, $\mathscr{R}$, de la taille des renforts, de la déformation de désaccord, du module élastique et de la résistance de la matrice. De plus, l'interface exerce une influence majeure sur la fissuration de la matrice, par une relaxation des contraintes par décohésion. En outre, les résultats impliquent qu'il existe une valeur de sécurité de $\mathscr{R}$, de l'ordre de l'unité, que l'one peut utiliser pour choisir des combinaisons de matériaux qui suppriment la fissuration de la matrice.

Zusammenfassung—Mit einer Kombination von Experiment und Rechnung wird der Bruch in einer spröden Verbundmatrix, hervorgerufen durch thermische Fehlpassung, behandelt. Es gibt eine kritische Größe der Verstärkungsteilchen, unterhalb der der Bruch der Matrix unterdrückt ist. Das Konzept wird zusammengefaßt mit einer nicht-dimensionalen Gruppe $\mathscr{R}$ aus Größe der verstärkenden Teile, Fehlpassungsverzerrung, elastischem Modul und Zähigkeit der Matrix. Außerdem wird gezeigt, daß die Grenzfläche einen größeren Einfluß auf die Rißbildung in der Matrix ausübt, indem die Bedingungen durch Aufreißen der Bindungen relaxiert werden. Des weiteren bedeuten die Ergebnisse, daß es einen bruchsicheren wert von $\mathscr{R}$ in der Größenordnung von eins gibt, mit dessen Hilfe Materialkombinationen ausgewählt werden können, in denen Rißbildung in der Matrix unterdrückt ist.

1. INTRODUCTION

In brittle intermetallic and ceramic matrix composites containing elastic reinforcements (particulates, fibers, platelets), thermal expansion mismatch can cause matrix cracking (Fig. 1). Such cracking adversely influences the structural performance of the composite and should be suppressed. Previous investigations of cracking around elastic inclusions [1–4] have recognized that the inclusion size is important, and that a *critical size, R_c, exists below which cracking does not occur*. Furthermore, dimensional analysis has suggested the existence of a non-dimensional group $\mathscr{R}$ defined as

$$\mathscr{R} = R(E_m \epsilon_T / K_m)^2 \qquad (1)$$

where R is the reinforcement size, K_m the matrix toughness, E_m the matrix modulus, and ϵ_T the misfit strain, given by

$$\epsilon_T = \int_{T_0}^{T} \Delta\alpha \, dT \qquad (2)$$

with $(T - T_0)$ being the processing temperature range and $\Delta\alpha$ the difference in thermal expansion coefficient between the matrix and the reinforcement (Fig. 2). The significance of this coefficient is that matrix cracking is found to be suppressed when *$\mathscr{R}$ is less than a critical value, $\mathscr{R}_c$. The magnitude of the cracking coefficient* $\mathscr{R}_c$ depends on the volume fraction f and aspect ratio of the reinforcements and on the ratio Σ of elastic modulus of the reinforcement to the matrix, as well as on the interface response (as exemplified by the friction coefficient μ).

The principal intent of the present study is to provide information about the magnitude of the cracking coefficient $\mathscr{R}_c$ for intermetallic matrices of practical interest ($MoSi_2$, γ-TiAl and $TiTaAl_2$) and thereby, to provide estimates of the critical reinforcement size R_c, needed to suppress matrix cracking. The material properties and processing conditions are summarized in Tables 1 and 2, and the calculated non-dimensional number $\mathscr{R}$ is given in Table 3.

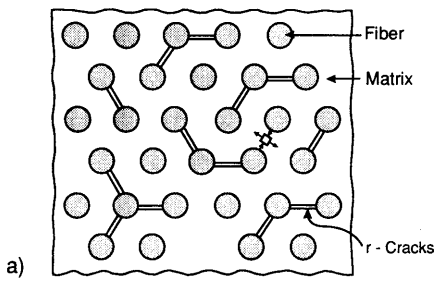

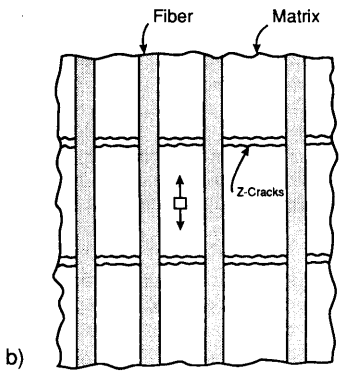

Fig. 1. A schematic illustrating the types of cracking caused by thermal expansion misfit. (a) r-cracks, (b) z-cracks.

In reinforced materials, several matrix crack morphologies are possible. These are defined here for clarity (Fig. 1). In aligned fiber composites, cross sections normal to the fiber axis reveal cracks that extend radially between fibers: these are referred to as *r-cracks*. In cross sections parallel to the fiber axis, periodic parallel cracks are observed having crack plane normal to the fiber axis: these are referred to as *z-cracks*. In other cases, interface cracks can form: these are termed *θ-cracks*. Previous calculations have addressed the incidence of z-cracks [5]. These studies have revealed that the critical size depends upon the response of the interface. For a well-bonded interface, the cracking coefficient $\mathscr{R}_c$ depends on f, Σ and the Poisson's ratio, v. Furthermore, when the elastic moduli are the same for both the fiber and matrix $\mathscr{R}_c$ has the form [5]

$$\mathscr{R}_c = \sqrt{6}B^2(1-v)^3(1+v)^{1/2}/f(1-f) \qquad (3)$$

where B is a coefficient between 0.8 and 1. The trend obtained by letting $B = 0.8$ and $v = 0.25$, is plotted on Fig. 3. However, fiber reinforced brittle matrix composites often require fiber coatings that induce *debonding* (and sliding) in the presence of matrix cracks [5, 6]. In this case, matrix cracking is *facilitated* and the friction coefficient of the debonded interface, μ, becomes an additional variable. For finite μ, the cracking coefficient becomes [5] ($\Sigma = 1$)

$$\mathscr{R}_c = 3\mu(1-v)/f. \qquad (4)$$

The behaviour obtained by letting $\mu = 0.1$, and $v = 0.25$, is plotted on Fig. 3. *The major influence of the interface response predicted by the calculations is an important theme of this article.*

The present study extends the above results for z-cracks to include r-cracks; a more commonly reported mode of matrix cracking. The investigation also involves experiments designed to explore the effects of misfit and of reinforcement size. The experiments are conducted primarily with $MoSi_2$ and γ-TiAl matrices containing various SiC and Al_2O_3 reinforcements, having the thermal expansion coefficients indicated on Fig. 2 and Table 1. Some experiments on $TiTaAl_2$ reinforced with W fibers are also reported [7]. A comparison of the thermal expansion coefficients (Fig. 2) indicates that the $MoSi_2/Al_2O_3$ system should be the least susceptible to

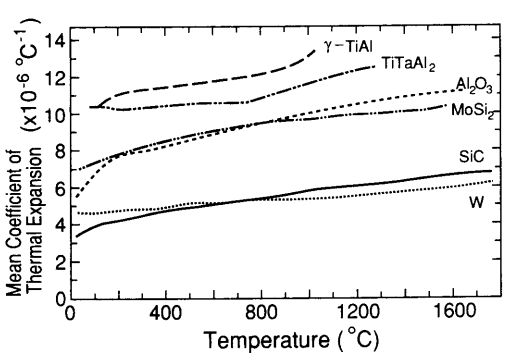

Fig. 2. Thermal expansion information for the materials of present interest.

Table 1. Property data for composite constituents

Material	K_c(MPa$\sqrt{m}$)	$\bar{\alpha}(10^{-6}K^{-1})$	E(GPa)
$MoSi_2$	4	9	400
γ-TiAl	8	12	170
$TiTaAl_2$	~8	11	190
SiC	3	5	420
Al_2O_3	4	9	400
W	~12	5	408

Table 2. Processing parameters

Composite	f	$2R$(μm)	ΔT(°C)
$MoSi_2$/SiC (SCS-6 fibers)	0.25	150	1330
$MoSi_2$/SiC (particulates)	0.42	68	1330
$MoSi_2$/SiC (platelets)	0.25	38	1330
$MoSi_2$/SiC (Nicalon fibers)	0.30	12	1330
$MoSi_2$/SiC (particulates)	0.42	12	1330
$MoSi_2$/SiC (whiskers)	0.25	1	1330
$MoSi_2/Al_2O_3$ (platelets)	0.20	38	1330
$MoSi_2/Al_2O_3$ (FP fibers)	0.50	20	1330
$TiAl/Al_2O_3$ (FP fibers)	0.10	20	1046
$TiTaAl_2$/W-3Re (fibers)	0.30	75	1180

Table 3. List of $\mathscr{R} = R(E_m\epsilon_T/K_m)^2$ values

Composite	Fibers	Platelets	Particulates	Whiskers
$MoSi_2/Al_2O_3$	0.01	0.02	—	—
$MoSi_2/SiC$	1.7 (Nicalon)		1.7 (12 μm)	
	21 (SCS-6)	5.4	9.6 (68 μm)	0.1
$TiAl/Al_2O_3$	0.04	—	—	—
$TiTaAl_2/W$–3Re	1	—	—	—

matrix cracking. However, the incidence of cracking in the other systems should reflect the importance of the parameters in equation (1) and be sensitive to reinforcement size and shape as well as the matrix toughness and the interface response.

2. CALCULATIONS

2.1. Stress distributions

The calculations are conducted with the objective of providing insight into the important trends as well as to give the approximate magnitudes of the cracking coefficient $\mathscr{R}_c$, especially for those systems with matrices having larger thermal expansion coefficient than the reinforcement (Table 1). For this purpose, elastic mismatch between the matrix and the reinforcement is neglected, i.e. the composite is taken to be *elastically homogeneous*. The thermal stress distributions prior to cracking are examined first in order to give some indication of possible fracture behaviors. The solutions also provide the basis for the evaluation of K.

Consider a single long fiber embedded in an infinite matrix. The stress field induced by the differential thermal straining is three dimensional in nature. This field may be obtained by the superposition of the two problems sketched in Fig. 4. In problem A, the system is subjected to thermal loading, as well as a mechanical compression at the ends, having magnitude

$$\sigma = E\epsilon_T/(1-\nu). \tag{5}$$

The fictitious compression is removed by superimposing problem B, which involves a tensile stress but *no* thermal straining. The following Lamé distribution is the *exact* solution to problem A

$$\begin{aligned}
&\sigma_r^f = \sigma_\theta^f = -\sigma/2,\\
&\sigma_z^f = -\sigma,\\
&\tau_{z\theta}^f = \tau_{r\theta}^f = 0.\\
&\sigma_r^m = -0.5\,\sigma(R/r)^2,\\
&\sigma_\theta^m = 0.5\,\sigma(R/r)^2,\\
&\sigma_z^m = \tau_{z\theta}^m = \tau_{r\theta}^m = 0
\end{aligned} \tag{6}$$

where the superscripts f and m signify the fiber and matrix, respectively. For the isolated fiber, the correction due to problem B is localized around the fiber ends. A force balance argument shows the correction at a distance z from one of the ends is of order, $(R/z)^2$, which is negligible when the fiber is long. Consequently, distribution (6) is an accurate solution to the original thermal mismatch problem. Important aspects of this solution are the diminishing σ_θ^m which implies that *r-cracks* emanating from the fiber should arrest in the matrix, and $\sigma_z^m = 0$ which implies that *z-cracks* are totally suppressed around an isolated fiber in an infinite matrix. In a finite matrix, σ_z^m would become non-zero and increase in magnitude as the ratio of the fiber-to-matrix volume increases. This characteristic is elaborated on below, in connection with solutions for finite fiber volume fraction.

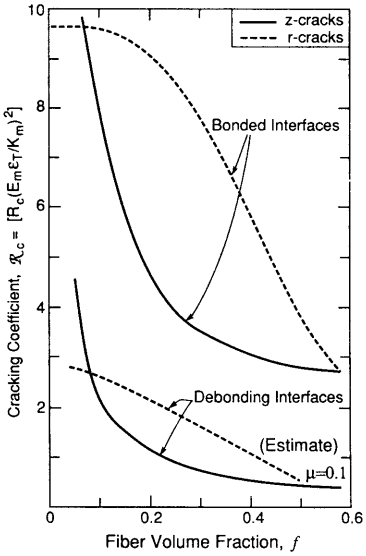

Fig. 3. Trends in the cracking coefficient with volume fraction for r-cracks and z-cracks with well-bonded interfaces and for interfaces that debond and slide readily: μ is the friction coefficient.

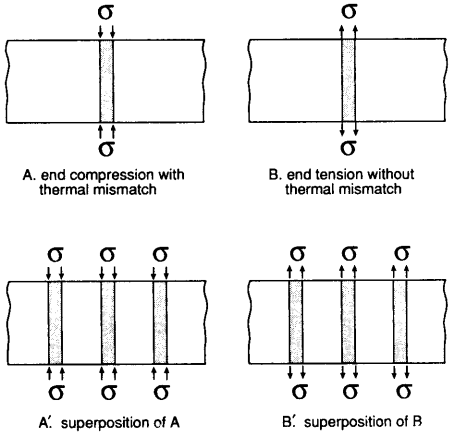

Fig. 4. A schematic of the supposition used to determine the many-fiber stress field prior to cracking.

The simplification that the composite is elastically homogeneous allows the many-fiber solution to be constructed by superposition (Fig. 4). As suggested by equation (6), problem A' does not contribute to the axial stress σ_z in the matrix. The fiber length is normally much larger than the fiber radius and spacing, and hence, the applied axial stress in problem B' can be homogenized as a uniform distribution, $f\sigma$. Consequently, the axial stresses are *uniform* in the matrix and in each of the fibers, respectively

$$\sigma_z^f = -(1-f)\sigma, \quad \sigma_z^m = f\sigma. \tag{7}$$

The stress components in the plane normal to the fibers, σ_r, σ_θ and $\tau_{r\theta}$, depend on the fiber distribution; a simple superposition can be programmed using the basic solution (6), since no in-plane contribution arises from problem B'. There are *no* shear stresses τ_{rz} and $\tau_{\theta z}$ except for the localized region around the fiber ends.

2.2. Cracking coefficients for r-cracks

2.2.1. Isolated fiber. A calculation of initial interest concerns a radial crack around an isolated fiber in an elastic matrix. Inserted into the configuration of Fig. 5 is a planar crack emanating from the fiber, which partially releases the hoop stress. The stress intensity factor at the advancing tip is obtained by integrating the hoop stress σ_θ^m in equation (6), by using the standard weight function for a through crack in an infinite plane. The normalized result depends on the relative flaw size, a/R, in accordance with [8]

$$K/\sigma\sqrt{R} = (\pi/8)^{1/2}(a/R)^{1/2}(1+a/R)^{-3/2} \tag{8}$$

as plotted on Fig. 5. Owing to the localized nature of the thermal stress distribution, K vanishes for long cracks and attains a maximum, $K_{max} = 0.24\,\sigma\sqrt{R}$, at the flaw size, $a/R = 0.5$. *The practical significance is that matrix flaws are incapable of developing into radial cracks provided the matrix toughness K_m satisfies $K_m > K_{max}$.* A rigorous bound for the avoidance of matrix cracking thus exists, leading to a definition of the cracking number

$$\mathscr{R}_c = 17.5(1-\nu)^2. \tag{9a}$$

In many cases, the matrix crack does not arrest at the interface, but debonds along the interface. Solution of this problem is complex, because the debond crack is mode II and also subject to frictional resistance. However, a lower bound for $\mathscr{R}_c$ may be provided by neglecting frictional effects and by assuming that the interface completely debonds. Then, the solution for a radial crack emanating from a hole subject to internal pressure [9] may be used to provide the estimate,

$$\mathscr{R}_c \approx 4(1-\nu)^2. \tag{9b}$$

A substantial effect of the interface response on the magnitude of $\mathscr{R}_c$ is apparent. Further calculations would be needed to examine the relaxation effects of debonding and sliding in detail.

2.2.2. Effects of volume fraction. The stress intensity factor for a matrix crack surrounded by many fibers can be obtained by superposition. The calculations utilize the solution to the kernel problem depicted in Fig. 6. The mode I stress intensity factor due to the single fiber is obtained by integrating the residual stress [equation (6)] prior to cracking [8]

$$K/\sigma\sqrt{R} = \sqrt{\pi/8}(a/R)^{1/2}(d_1/R)^{-1/2} \times (d_2/R)^{-3/2}\cos(\theta_1/2 + 3\theta_2/2). \tag{10}$$

The lengths d_i and angles $\theta_i (i = 1, 2)$ are defined in Fig. 6. The θ_i-dependence suggests fibers that are located above and below the crack give negative K and therefore tend to close the crack.

To explore the effects of volume fraction and of fiber proximity, calculations have been conducted for several fiber arrangements with a strong interface. Both cubic and hexagonal arrays have been used, as well as two isolated fibers. Representative results obtained for fixed fiber spacing, $L/R = 3$ (Fig. 7), which corresponds to a fiber volume fraction, $f \approx 0.4$, indicates that in all cases K increases monotonically, rather than exhibiting a maximum. Consequently, the critical size is now subject to some *a priori* knowledge of flaws present in the matrix. The important trends

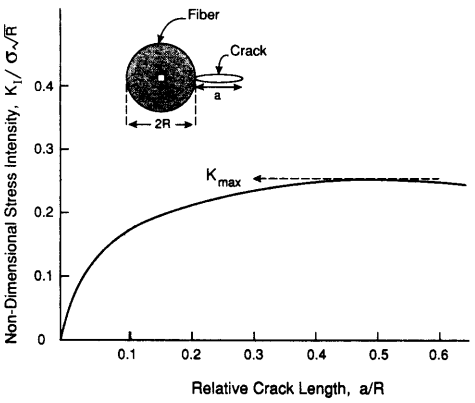

Fig. 5. Trends in non-dimensional stress intensity factor with r-crack length for an isolated fiber with a well-bonded interface.

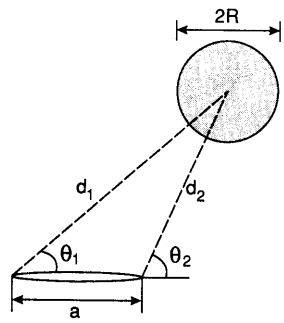

Fig. 6. A schematic of the kernel problem used to calculate stress intensity factors induced by many fibers.

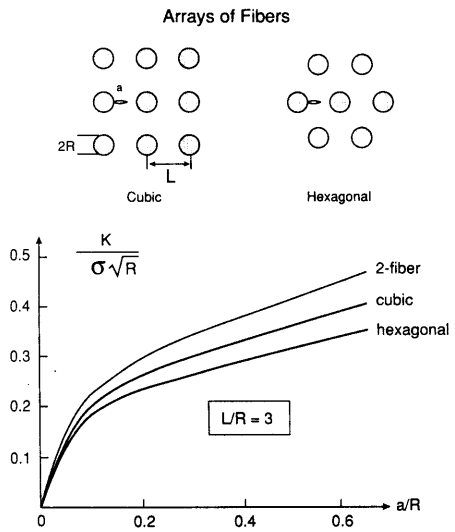

Fig. 7. Variations in K with crack length for r-cracks in various fiber arrangements.

in matrix cracking can be illustrated by using an arbitrary choice of the matrix flaw size, $a_0 = 0.5R$ (the magnitude of the maximum for the isolated fiber, Fig. 5). With this choice, trends in $\mathscr{R}_c$ are plotted on Fig. 3, and discussed below.

Comparison of the results for r- and z-cracks (Fig. 3) indicates that the latter have a stronger dependence on volume fraction, and that r-cracks are more likely for $f \lesssim 0.1$ and z-cracks for $f \gtrsim 0.1$. The important effect of the interface on $\mathscr{R}_c$ (Fig. 3) is illustrated by assuming that the volume fraction dependence of the incidence of r-cracks with unbonded interfaces is comparable to that ascertained for bonded interfaces. The effects of fiber spatial arrangement (Fig. 7) suggest that cracking is more likely with fibers having a cubic, rather than a hexagonal array. Cracking is also more likely between two fibers that have a spacing smaller than the average value for the array. *However, the effects of spatial arrangement are smaller than the influence of the interface.*

Despite the significant influences on $\mathscr{R}_c$ of the interface, as well as the reinforcement volume fraction and the spatial arrangement, some broad guidelines emerge. *Notably, it is apparent from Fig.* 3 *that all forms of cracking should be suppressed provided that* $\mathscr{R} < 1$. Conversely, profuse matrix cracking should be expected when $\mathscr{R} > 10$.

3. EXPERIMENTAL

3.1. Processing

All composite systems were made using a powder metallurgy approach with consolidation achieved by hot isostatic pressing. The materials properties and processing parameters are summarized in Tables 1 and 2. The systems reinforced with platelets of either SiC or Al_2O_3 were produced by mechanical blending of the matrix powder with the reinforcements. The blended powders were inserted into either a Nb or a Ti can which was then evacuated and sealed. Thereafter, HIPing to full density was conducted using a pressure of 276 MPa and a temperature of either 1350°C for $MoSi_2$ or 1066°C for TiAl, applied for ~2 h. The fiber reinforced materials were processed by drawing the fiber through a slurry of matrix powder mixed with an organic binder to form a monotape. The tapes were then stacked and the binder removed by calcination. Consolidation was achieved by hot isostatic pressing.

3.2. Observations and comparisons

The results of the observations are compared with the calculations in Fig. 8. All observations have been made on polished cross sections of the composites, using electron microscopy. In some cases, the cross-sections were etched to reveal the microstructure of the matrix. The first set of observations establishes the lack of matrix cracking in the $MoSi_2/Al_2O_3$ system (Fig. 9). Matrix cracks could not be detected even at the ends of platelets or between closely spaced fibers. The calculations suggest that the most critical configuration for the incidence of matrix cracking in this system should be z-cracking in regions containing high volume fractions of fibers [Fig. 9(c)]. Furthermore, since $MoSi_2$ and Al_2O_3 exhibit strong bonding, by means of the formation of a mullite interphase (Fig. 9), the calculations for the bonded interface are most applicable. These calculations give a critical cracking coefficient $\mathscr{R}_c \approx 3$ for $f \approx 0.5$. Based on the information in Tables 1 and 2, $\mathscr{R}$ is <0.03. Hence, $\mathscr{R} \ll \mathscr{R}_c$ *consistent with the absence of matrix cracks.*

A second set of observations, obtained for $MoSi_2$ reinforced with SiC, validates the existence of a critical size below which matrix cracking is suppressed, and that this size coincides with $\mathscr{R}$ of order unity. Specifically, extensive r-cracking is evident in composites with large fiber or particulate/platelet reinforcements (Fig. 10a,b,c), but could not be detected in composites with whiskers [Fig. 10(f)]. The small diameter (12 μm) Nicalon fiber composites seem to be on the borderline with respect to matrix cracking, with a few hairline cracks between some, but not all the fibers [Fig. 10(d)]. Cracking is also observed in large particulate [Fig. 10(b)] and platelet [Fig. 10(c)] reinforced composites, while a composite with relatively small particulates (~12 μm) did not crack (Fig. 10(e)]. It is also apparent that, wherever large matrix cracks intercept the reinforcements, interface debonding occurs [Fig. 10(a)]. The cracking coefficients are thus assessed for interfaces subject to debonding. However, since the friction coefficient is unknown for this interface, two limiting values ($\mu = 0.1$ and $\mu = 0.5$) are used on Fig. 8(b) to compare experiments with theory; the respective r-crack predictions are an estimation from the system with bonded interfaces. Consequently, since f is in the range 0.2–0.4 in each case, $\mathscr{R}_c \approx 1$ for $\mu = 0.1$.

Comparison between calculated $\mathscr{R}$ (Table 3) and this value fo $\mathscr{R}_c$ [Fig. 8(b)] confirms r-cracking in the materials with large (150 μm) fibers ($\mathscr{R} \approx 21$), with large (68 μm) particulates ($\mathscr{R} \approx 9.6$) or with large (38 μm) platelets ($\mathscr{R} \approx 5.4$) and with small (12 μm) fibers ($\mathscr{R} \approx 1.7$), as well as the absence of cracking in the whisker reinforced material ($\mathscr{R} \approx 0.1$). The absence of z-cracks in the material with small diameter fibers and in the whisker containing material is also consistent with the prediction, subject to the uncertainty in μ. Moreover, all the calculations were conducted for composites reinforced with fibers, hence, comparisons between platelet or particulate reinforced composites and the predictions are not strictly valid. Nevertheless, the trends for matrix cracking as a function of particle size are in the right direction with only the finer particulate (23 μm) composite exhibiting no matrix cracks.

Further confirmation of the analysis is provided by results on the $TiAl/Al_2O_3$ and $TiTaAl_2/W$–3 wt% Re systems. The former exhibits no detectable cracking for $f \approx 0.1$ (Fig. 11). Moreover, independent experiments indicate good interface bonding [10]. Consequently, based on the property data in Table 1, $\mathscr{R} \approx 0.04$, whereas $\mathscr{R}_c \approx 8$, *consistent with the absence of both z- and r-cracks.* For W–3Re in $TiTaAl_2$, z-cracks form [Fig. 12(a)] and moreover, debonding occurs, because an Al_2O_3 fiber coating has been used [Fig. 12(b)]. For this case $f \approx 0.3$, $\mathscr{R} \approx 1$ and $\mathscr{R}_c \approx 0.7$, *consistent with the incidence of z-cracks* [Fig. 8(b)].

A feature of the above comparisons has been the importance of the interface response to the selection

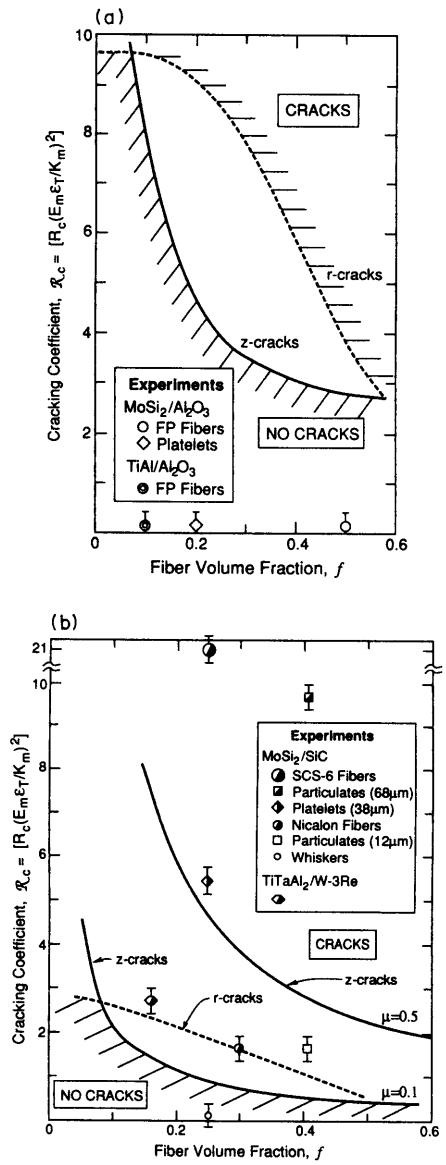

Fig. 8. Comparison between observations and predictions. (a) Systems with bonded interfaces: None of the systems exhibit either r- or z-cracks. (b) Systems with debonding interfaces: cracks have not been found for $MoSi_2$-SiC with either whiskers or small particulates: cracks have been detected in other cases. However, the crack density is relatively low for $MoSi_2$ with Nicalon fiber reinforcements.

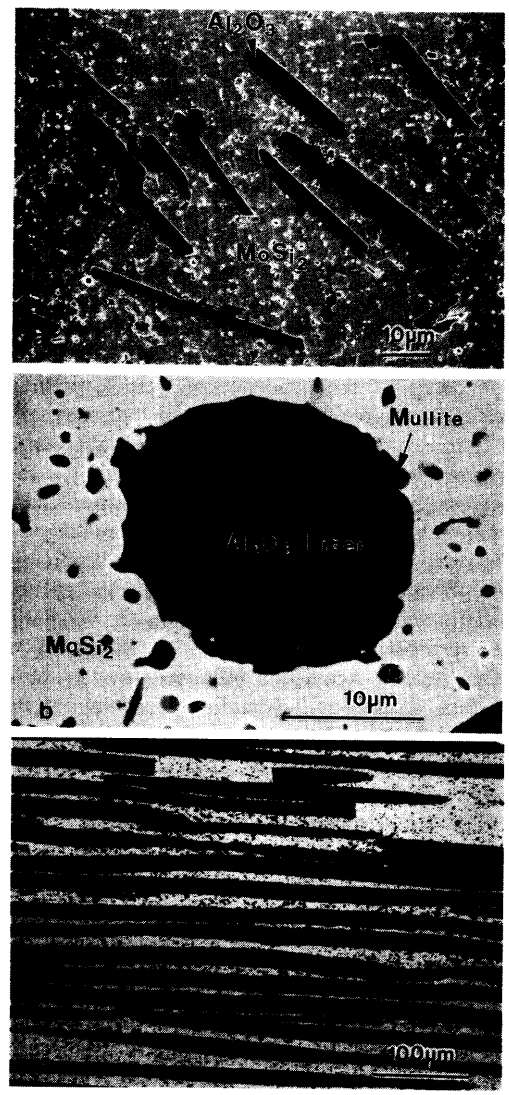

Fig. 9. SEM views of polished and etched sections of composites in the $MoSi_2/Al_2O_3$ system. (a) Platelets, (b) FP fibers: transverse, (c) FP fibers: longitudinal.

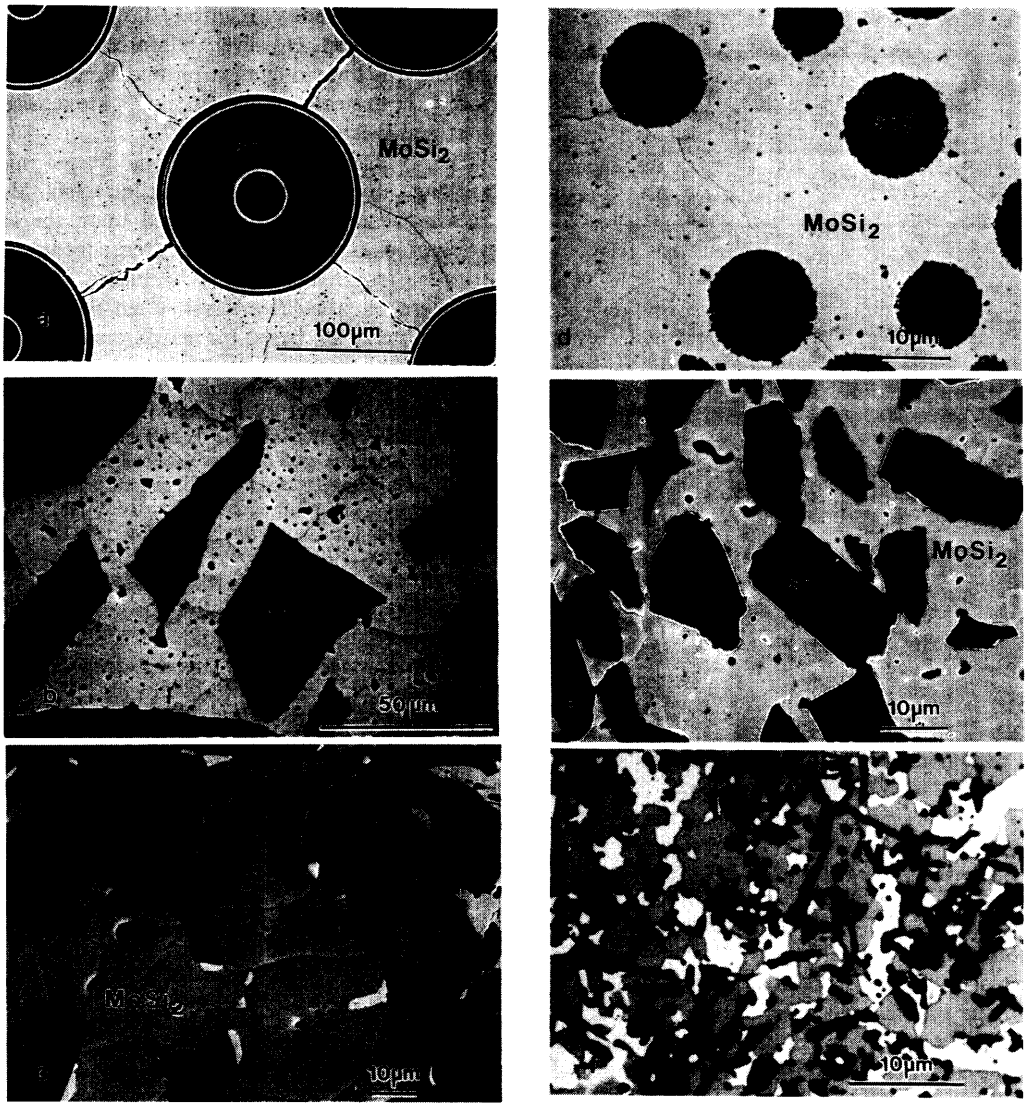

Fig. 10. SEM views of polished sections of composites in the $MoSi_2$/SiC system (the white phase is Mo_5Si_3): (a) AVCO SCS-6 fibers, (b) particulates (68 μm) (c) platelets (38 μm), (d) Nicalon fibers, (e) particulates (12 μm), and (f) whiskers.

of $\mathscr{R}_c$ and hence, on the consistency between experiment and theory. Notably, a substantially greater tendency for matrix cracking is found for systems wherein the interface debonds readily.

4. CONCLUDING REMARKS

The incidence of matrix cracking in brittle matrix composites induced by thermal expansion misfit between the reinforcement and matrix has been shown to be characterized by a non-dimensional cracking coefficient, $\mathscr{R}$. The magnitude of $\mathscr{R}$, is governed by the misfit strain, by the matrix toughness and modulus and by the reinforcement size. A broad characterization has further revealed that matrix cracking is generally suppressed when $\mathscr{R} < 1$, whereas profuse cracking is expected where $\mathscr{R} \gtrsim 10$. Cracking sensitivity within the $\mathscr{R}$ range between 1 and 10 is strongly influenced by interface debonding, in the sense that *debonding encourages matrix cracking*. Cracking also

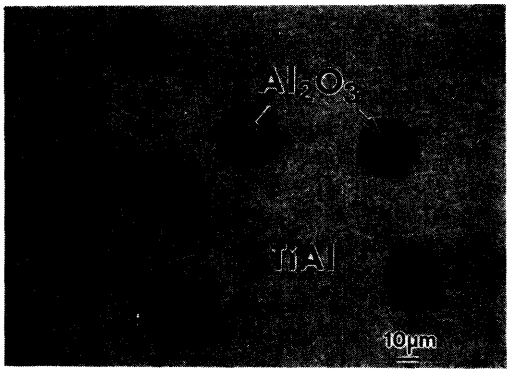

Fig. 11. SEM views of a polished cross-section of a γ-TiAl matrix reinforced with FP Al_2O_3 fibers.

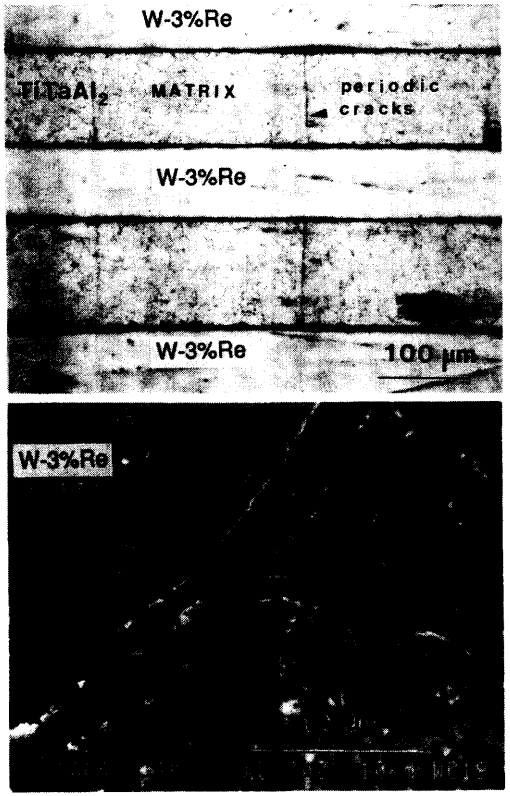

Fig. 12. (a) z-cracks in a $TiTaAl_2$ composite reinforced with W–3 wt% Re fibers, (b) debonding between the Al_2O_3 coating and the W–3 wt% Re fiber.

becomes more likely as the reinforcement volume fraction increases.

To place the above characteristics in context, the role of the interface on other properties of importance is discussed. When the reinforcements are used for creep resistance, good interface bonding is required. Consequently, relatively large values of $\mathscr{R}$ may be tolerated. However, reinforcements used to improve fracture toughness must debond and slide readily. In this case, small values of $\mathscr{R}$ are required to avert matrix cracking.

The preceding research has addressed matrix cracking caused by thermal expansion misfit. Matrix cracking tendencies are enhanced upon the application of loads to the composite. Consequently, more stringent requirements must be placed on $\mathscr{R}$ and hence, on the allowable misfit, when the composite design criteria are based on matrix cracking.

Acknowledgements—The support of the Defense Advanced Research Projects Agency (DARPA) through a contract MDA972-90-K-0001, supervised and monitored by Dr William Barker, is gratefully acknowledged. The authors would like to thank Y. G. Deng for preparation of some of the specimens. The work of Z. Suo is partially supported by a NSF research initiative award (MSS-9011571).

REFERENCES

1. R. W. Davidge and T. J. Green, *J. Mater. Sci.* **3,** 629 (1968).
2. Y. M. Ito, M. Rosenblatt, L. Y. Cheng, F. F. Lange and A. G. Evans, *Int. J. Fract.* **17,** 483 (1981).
3. A. G. Evans, *J. Mater. Sci.* **9,** 1145 (1974).
4. F. F. Lange, *Fracture Mechanics of Ceramics*, Vol. 2, p. 599. Plenum, New York (1976).
5. B. Budiansky, J. W. Hutchinson and A. G. Evans, *J. Mech. Phys. Solids* **34,** 167 (1986).
6. A. G. Evans and D. B. Marshall, *Acta metall.* **37,** 2567 (1989).
7. H. Dève and M. Maloney, *Acta metall. mater.* To be published.
8. Z. Suo, *Int. J. Solids Struct.* **25,** 1133 (1989).
9. B. Budiansky, A. G. Evans and R. Mehrabian, unpublished work.
10. M. L. Emiliani, R. J. Hecht, H. E. Deve, J. B. Davis and A. G. Evans. To be published.